Characterization and decoration of the two-dimensional Penrose lattice

Vijay Kumar and Debendranath Sahoo
Materials Science Laboratory, Indira Gandhi Centre for Atomic Research, Kalpakkam 603 102, Tamilnadu, India

G. Athithan
Computer Centre, Indira Gandhi Centre for Atomic Research, Kalpakkam 603 102, Tamilnadu, India
(Received 3 February 1986)

The self-similarity property of the two-dimensional Penrose lattice is utilized to characterize it in terms of the distribution of different kinds of vertices, the Voronoi cells, and their nearest neighborhoods. Striking similarities are observed between the layer structures of the crystalline δ-$Al_{11}Mn_4$, Al_6Mn, $Al_{13}Fe_4$, Pt_5P_2, and Ni_3Si_2 with a sublattice of the Penrose lattice. The latter can be described in terms of cells which need not have fivefold rotational symmetry. Following the atomic distributions in the crystalline Al_6Mn and $Al_{13}Fe_4$, decorations of such lattices are suggested to model the T phase of Al-Mn and other related quasicrystals. We find two types of layers with fivefold rotational symmetry in the T phase. This is in agreement with the electron diffraction from such quasicrystals.

I. INTRODUCTION

Recent discovery of rapidly cooled Al-Mn alloys[1] with icosahedral symmetry has posed a challenging crystallographic problem for the characterization of this new phase of condensed matter now known as the i phase or quasicrystal. As revealed by electron diffraction,[1] these alloys have long-range bond-orientational order but lack translational periodicity as one should expect in the presence of fivefold rotational symmetry. Such quasiperiodic structures can be generated[2] from two or more (but finite) number of unit cells[3] (repeating motifs). This phase therefore represents a state between crystalline and glassy materials, which have one and an infinite number of unit cells, respectively. While the sharp fivefold diffraction pattern has been readily understood[4–6] in terms of the structure factor of the bare Penrose lattice (PL), several models[7–11] have been proposed for the relative positions of Al and Mn atoms in these alloys. Of these the ones proposed by Guyot and Audier[8] and Elser and Henley[11] hold some promise. Both of these describe essentially the same basic packing unit and are based on the α-(Al-Mn-Si) crystalline structure. But in their model[8] it still remains to completely identify the positions of Al atoms. From earlier Mössbauer[12] and extended x-ray-absorption fine structure[13] (EXAFS) experiments, presence of two types of Mn sites with their relative concentration in the ratio of the golden mean $\tau=(\sqrt{5}+1)/2$ was inferred as also in the model of Guyot and Audier. However, in a recent Mössbauer study[14] it is concluded that there are several types of Mn neighborhoods as in an amorphous solid and therefore the situation still remains unclear.

In addition to the i phase, these alloys also form a decagonal phase[15,16] (also known as the T phase) when cooling rates are lower or the Mn concentration is increased. In this phase a periodic packing of two-dimensional (2D) quaiscrystals occurs. Interestingly several crystalline compounds, including the ones forming quasicrystals, have layered structure and in many cases there are pentagon-tetragon-triangle nets.[17] As we shall show, these have striking resemblance to a sublattice generated from the 2D PL (Ref. 18) with "thin" and "fat" rhombi [with angles $(\pi/5,4\pi/5)$ and $(2\pi/5,3\pi/5)$ respectively] as their unit cells. Obviously as in Refs. 8 and 11, the study of the crystalline structures together with the 2D PL can give some clues regarding the atomic distributions in the T phase. Moreover, the 2D PL is a section through a three-dimensional (3D) PL and high-resolution electron micrographs with fivefold symmetry have been interpreted[19] in terms of the decorations of the 2D PL. Therefore the decorations of the 2D PL which are much easier to visualize than the 3D PL may even prove helpful in understanding further the atomic distribution in the i phase as well as the correlation between the T phase and the i phase if any exists.

Though the original Penrose tiling were developed[2] in two dimensions, most attention (see, e.g., Refs. 4–6) has been focused on the study of the 3D PL after the discovery of Al-Mn and other quasicrystals. In this paper we study the 2D PL. Unlike the regular lattices, different lattice points of a PL have different local neighborhoods and hence their characterization is nontrivial. We have used the self-similarity property of the 2D PL (Ref. 20) to calculate concentrations of different vertices and the conditional probabilities of the neighborhoods of a given vertex. This information can be used to generate ordered arrangements of atoms (with a given concentration of different species) by decorating the Voronoi cells. The Voronoi construction[21] of the 2D PL is a "froth"[22] and exhibits pentagons and heptagons in addition to hexagons. The numbers of pentagons and heptagons turn out to be equal and therefore the average coordination of a Voronoi cell is six, as should be expected for a "froth." However, it will be shown that in actual 2D quasicrystals which can be modeled with the PL as the underlying lattice, the number

of atoms having five and seven neighbors need not be equal, as some of the cells may remain unoccupied. Moreover, coordinations other than 5, 6, and 7 can be generated so that in general the average coordination for a decorated 2D PL need not be six and may even turn out to be a noninteger.

Our decorations of the 2D PL are based upon the atomic arrangements in the layers of Al_6Mn and $Al_{13}Fe_4$ (which has the same structure as Al_3Fe) compounds. The close relationship of the crystalline compounds with the decagonal phase of Al-Mn can further be noted from the fact that the repeat distances normal to the layers in Al_4Mn, Al_3Mn, and Al_3Fe compounds are[11] 12.4, 12.59, and 12.476 Å whereas in the decagonal phase of Al-Mn alloys it is[15] 12.4 Å. We shall show that similar to the Al_3Fe compound, there are two types of layers in the decagonal phase. This agrees with the results of diffraction patterns[15] of the Al-Mn decagonal phase along the twofold axes (normal to the fivefold axis).

In Sec. II we discuss the distribution of vertices and their neighborhoods in the 2D PL and in Sec. III we describe its decorations for Al-Mn, Al-Fe, and related quasicrystals. Section IV presents a brief summary of the work.

II. CHARACTERIZATION OF THE 2D PENROSE LATTICE

We consider here the arrowed rhombus tiling of a plane [Fig. 1(a)] as discussed by de Bruijn.[18] This belongs to the Penrose local isomorphic[23,24] (PLI) class. Although in real quasicrystals deviation from such a tiling may occur, the PLI class is the most interesting for the present purpose. As discussed by de Bruijn,[18] there are eight kinds of vertices on this tiling and these are denoted by D, J, Q, K, $S3$, $S4$, S, and $S5$ (Table I). From the self-similarity property of the PL it is possible to introduce sublattices.[25] Like the regular lattices, these sublattices will in general have unit cells differing from the original ones. In the present case, consider a given PL, for example, $(PL)_0$. Let $(PL)_1$ be the inflated[26] PL obtained from $(PL)_0$. The side of each rhombus in $(PL)_1$ is τ times that of $(PL)_0$. The process of inflation is described in detail by de Bruijn.[18]. The vertices of $(PL)_1$ consist of a fraction $1/\tau^2$ of those of $(PL)_0$. Let the vertices of $(PL)_n$ be denoted by a subscript n, like D_n, $(S3)_n$ etc. ($n=0,1,2,\ldots$). In the transition $(PL)_0\rightarrow(PL)_1$, $D_0\rightarrow 0$ and $J_0\rightarrow 0$; i.e., these vertices are suppressed. Also $Q_0\rightarrow D_1$, $K_0\rightarrow J_1$, $(S3)_0\rightarrow Q_1$, $(S4)_0\rightarrow K_1$, $S_0\rightarrow(S3)_1+(S4)_1+(S5)_1$, and $(S5)_0\rightarrow S_1$. Here the reader is advised to consult Table I for identifying the vertices of $(PL)_0$ and $(PL)_1$ in Fig. 1(a), which exhibits this transition clearly. The D_0 and J_0 vertices together constitute a tetracoordinated sublattice of $(PL)_0$ (see Fig. 2). This pattern is very similar to the one derived by Mosseri and Sadoc,[27] who obtained it by a suitable decoration of the "kite" and "dart" Penrose pattern.[2] It is easy to notice that this sublattice has identical 20-gons which overlap with each other. Each 20-gon has a mirror but no rotational symmetry. However, there is a point of global fivefold rotational symmetry (not seen in the figure) and as one can see *to produce a pattern with a pentagonal symmetry it is not necessary to use only the polygons which have fivefold rotational symmetry or whose angles are integral multiples of $\pi/10$* in contrast to models of *i* phase where packing of only the icosahedra has been considered. The sublattice depicted in Fig. 2 appears to be important for quasicrystals of alloys whose crystalline structure is based on pentagon-tetragon-triangle nets.[17] Apart from this sublattice, there are three other sublattices in the 2D PL. In order to see how these sublattices arise, let us denote by $(PL)_n$ the inflated PL obtained from $(PL)_{n-1}$ ($n=1,2,3,\ldots$). The transition

$$(PL)_0\rightarrow(PL)_1\rightarrow(PL)_2\rightarrow(PL)_3\rightarrow\cdots$$

is described by the following transformations of vertices:

$$D_0\rightarrow 0\,,\quad J_0\rightarrow 0\,,\quad Q_0\rightarrow D_1\rightarrow 0\,,\quad K_0\rightarrow J_1\rightarrow 0\,,$$
$$(S3)_0\rightarrow Q_1\rightarrow D_2\rightarrow 0\,,\quad (S4)_0\rightarrow K_1\rightarrow J_2\rightarrow 0\,, \tag{1}$$
$$S_0\rightarrow\begin{cases}(S3)_1\rightarrow Q_2\rightarrow D_3\rightarrow\cdots\\(S4)_1\rightarrow K_2\rightarrow J_3\rightarrow\cdots\\(S5)_1\rightarrow S_2\rightarrow\begin{cases}(S3)_3\rightarrow\cdots\\(S4)_3\rightarrow\cdots\\(S5)_3\rightarrow\cdots\end{cases}\end{cases},$$
$$(S5)_0\rightarrow S_1\rightarrow\begin{cases}(S3)_2\rightarrow Q_3\rightarrow\cdots\\(S4)_2\rightarrow K_3\rightarrow\cdots\\(S5)_2\rightarrow S_3\rightarrow\cdots\end{cases},$$

Just as in the transition $(PL)_0\rightarrow(PL)_1$, the subset of vertices (D_0,J_0) drops out and constitutes a sublattice of $(PL)_0$, the subset consisting of (Q_0,K_0) drops out in $(PL)_2$, and similarly the subset consisting of $((S3)_0,(S4)_0)$ drops out in $(PL)_3$. From there on, S and $S5$ keep on interchanging in successive inflations $(PL)_n\rightarrow(PL)_{n+1}$, $n\geq 3$. In this manner, we obtain four sublattices[28] of a given PL consisting of the vertex pairs (D,J), (Q,K), $(S3,S4)$, and $(S,S5)$. The first three sublattices are similar (Fig. 2), but are progressively bigger and bigger in size by a factor τ (in linear dimensions) from the previous one. The fourth sublattice with S and $S5$ is similar to the starting PL but scaled by a factor τ^3. It is worth noting that the transformation of vertices upon inflation $(PL)_{n-1}\rightarrow(PL)_n$ can be expressed in a matrix form:

$$\begin{pmatrix}D_n\\J_n\\Q_n\\K_n\\(S3)_n\\(S4)_n\\S_n\\(S5)_n\end{pmatrix}=\begin{bmatrix}0&0&1&0&0&0&0&0\\0&0&0&1&0&0&0&0\\0&0&0&0&1&0&0&0\\0&0&0&0&0&1&0&0\\0&0&0&0&0&0&1&0\\0&0&0&0&0&0&1&0\\0&0&0&0&0&0&0&1\\0&0&0&0&0&0&1&0\end{bmatrix}\begin{pmatrix}D_{n-1}\\J_{n-1}\\Q_{n-1}\\K_{n-1}\\(S3)_{n-1}\\(S4)_{n-1}\\S_{n-1}\\(S5)_{n-1}\end{pmatrix}, \tag{2}$$

which can be written as

TABLE I. Classification of vertices and Voronoi cells for the arrowed rhombus Penrose lattice. The probabilities of vertices, the area of Voronoi cells, and their nearest neighborhoods are also given. $\tau=(\sqrt{5}+1)/2$, $A=1/[4\tau^2(1+\tau^2)^{1/2}]$ and a is the side of the rhombus. nV denotes n vertices of type V.

Vertex								
Voronoi cell								
de Bruijn's notation	D	J	Q	K	$S3$	$S4$	S	$S5$
$p(V)$	$\frac{1}{\tau^2}$	$\frac{1}{\tau^3}$	$\frac{1}{\tau^4}$	$\frac{1}{\tau^5}$	$\frac{1}{\tau^6}$	$\frac{1}{\tau^7}$	$\frac{1}{\tau^4(1+\tau^2)}$	$\frac{1}{\tau^6(1+\tau^2)}$
Cell area (units of a^2)	$(8\tau+3)A=0.8004$	$(9\tau+4)A=0.9319$	$(5\tau+4)A=0.607$	$(5\tau+7)A=0.7576$	$(7\tau+6)A=0.8698$	$2(3\tau+4)A=0.8890$	$5(2+\tau)A=0.908$	$5(2+\tau)A=0.908$
Neighborhood of a cell	(a) $Q,S,2D,S3,J$ (b) $K,S,2D,2J$ (c) $Q,K,D,S4,2J$ (d) $Q,K,D,S3,2J$	(a) $2K,4D,S3$ (b) $Q,K,3D,S4,J$ (c) $2Q,2D,S4,2J$ (d) $2Q,2D,S5,2J$	(a) $2D,S4,2J$ (b) $2D,S3,2J$	$3D,2J$	$2Q,4D,J$	$Q,2D,3J$	$5D$	$5J$
Probability distribution of neighborhoods (i)–(iv)	(a),(b) $2/\tau^4$ (b) $1/\tau^3$ (c) $2/\tau^5$ (d) $2/\tau^4$	(a) $1/\tau^3$ (b) $2/\tau^4$ (c) $1/\tau^4$ (d) $5/(1+\tau^2)\tau^3$	(a) $1/\tau^3$ (b) $2/\tau^2$	1	1	1	1	1

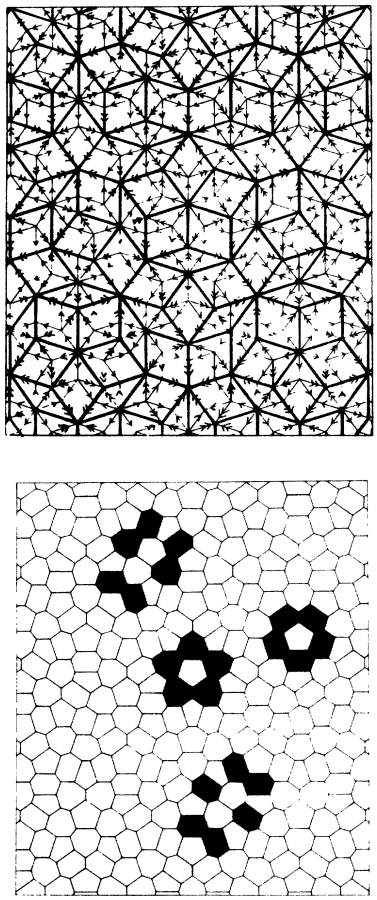

FIG. 1. (a) Arrowed rhombus Penrose lattice. Thick lines correspond to the first inflation. (b) The Voronoi construction corresponding to (a). The shaded polygons show the neighborhoods of vertices $S3$, $S4$, $S5$, and S (for details see also Table I).

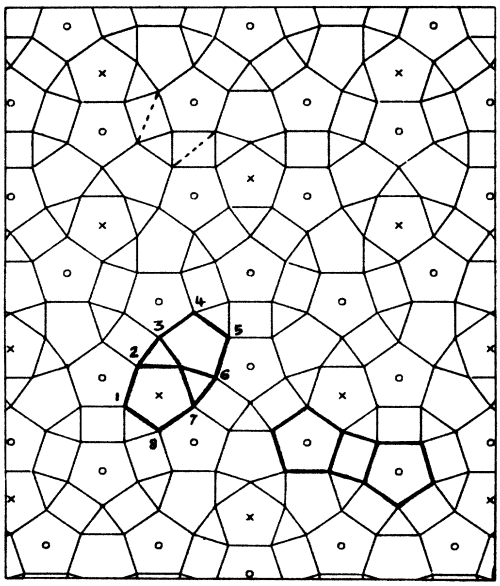

FIG. 2. The tetracoordinated network generated from D and J vertices. Circles denote vertices $S3$, $S4$, and $S5$, while a cross represents the vertex S. The hexagonal arrangement of Al atoms found in δ-$Al_{11}Mn_4$ or Al_6Mn (Fig. 3) is identified by drawing the two broken lines. The polygons with thick lines are found in structures shown in Fig. 4.

$$\underline{V}_n = \underline{M}\underline{V}_{n-1} \,. \tag{3}$$

Here $\underline{V}_{n-1}$ denotes the vertices on the starting PL whereas $\underline{V}_n$ denotes the vertices on the inflated PL. The transfer matrix $\underline{M}$ has some similarity with the transfer matrix of the fractals considered by Mandelbrot *et al.*[29] for the triadic Sierpinski carpet. In fact, the self-similarity property of the PL can be used to generate fractal trees with dimensionality $\ln 2/\ln\tau$ by keeping only the short diagonals of the thin rhombi on each deflation.[30] The transfer matrix corresponding to deflation is $\underline{M}^T$.

It is clear that D and J are not converted into any vertex upon inflation [see Fig. 1(a)]. J lies inside each inflated fat rhombus while a D originates from the two sides of each narrow rhombus of the starting pattern and lies on a side of the inflated fat rhombus. Upon inflation the number of rhombi of each type is $1/\tau^2$ times their number on the starting pattern. Since the number ratio of fat to thin rhombi is τ, it follows that the number of D vertices will be τ times that of J vertices. Also the number of vertices in a pattern is the same as the number of polygons. Therefore if the probabilities of different vertices $p(V)$ are normalized to unity, then from the fact that D and J are left out on inflation, we get $p(D)=1/\tau^2$ and $p(J)=1/\tau^3$. Also from Eq. (2) we have

$$p(D)=\tau^2 p(Q),\quad p(J)=\tau^2 p(K)\,,$$
$$p(S5)+p(S4)+p(S3)=\tau^2 p(S),\quad p(Q)=\tau^2 p(S3)\,,$$
$$p(K)=\tau^2 p(S4),\quad p(S)=\tau^2 p(S5)\,.$$

These can be solved immediately to obtain the concentrations of different vertices and these are listed[30(a)] in Table I. From these the average nearest-neighbor coordination $\bar{Z}$ of a vertex turns out to be 4,[31]

$$\bar{Z}=\sum_i Z_i p(i)\,, \tag{4}$$

where Z_i is the coordination of a vertex of type i. The same result follows also from Euler's equation,[32] which for an infinite $2D$ network is given by

$$\frac{1}{\bar{r}}+\frac{1}{\bar{n}}=\frac{1}{2}\,, \tag{5}$$

where $\bar{r}$ is the average number of edges meeting at the vertices and $\bar{n}$ is the average number of edges of the faces. Since in our case both types of faces (rhombi) have four edges, $\bar{n}=4$ and hence $\bar{r}=4$. The same will be true for a PL based on the "kite" and "dart" pattern[2] and also for the defective PL (Ref. 33) as well as other lattices in the PLI class, since the basic units are the same. This calculation is based upon the connectivity of different vertices, as shown in Fig. 1(a). However, if we consider the short diagonals of the two rhombi also to be among the nearest neighbors, then from Eq. (4) the average coordination is six. This is interesting as we shall see that the Voronoi construction has the mean coordination 6.

The Voronoi construction corresponding to the PL of Fig. 1(a) is shown in Fig. 1(b). It contains pentagons, hexagons, and heptagons only. Table I displays the polygons originating from different vertices. There are three types of pentagons, two types of hexagons, and two

types of heptagons. The relative abundances of pentagons and heptagons are equal and given by $2/\tau^4$. Hence the average coordination of each Voronoi cell is six. Since Voronoi construction is tricoordinated, the same result follows again from Eq. (5). The even and the odd central moments of the edge distribution defined[21] as

$$\mu_k = \sum_n (n-6)^k p(n) \tag{6}$$

are $4/\tau^4$ and 0, respectively. Here $p(n)$ is the probability of cells with n edges. Therefore the distribution is symmetric with width $4/\tau^4$. Since the histogram displaying the number of polygons with different number of sides in the Voronoi construction of the PL is symmetric about hexagons, the pattern is statistically free of disclinations although locally disclinations, dislocations (5-7 pairs), and grain boundaries [(5-7)—(5-7)— $\cdots$ strings] can always be found [see Fig. 1(b)]. Here the defects are defined[34] in the sense of the "5-7 construction" used extensively in the study of 2D systems. In the case of a general quasiperiodic lattice not belonging to the PLI class, nine additional types of vertices are possible[35] and the polygons associated with these new vertices will also have eight, nine, or ten sides. Though the Voronoi construction still remains tricoordinated (i.e., it still retains the "froth" property), the histograms of polygons will no longer remain symmetric about hexagons.

The neighborhood of each Voronoi cell in the PLI class is given in Table I together with their (conditional) probabilities. These were calculated from the knowledge of $p(i)$ and by visual inspection of a large Voronoi pattern of the PL. Katz and Duneau[35] and Elser[4] have developed a general mathematical procedure for the calculation of neighborhood patterns in a PL in arbitrary dimensions but the details of the neighborhoods of the 2D PL are not given. It is noted that the vertices K, $S3$, $S4$, S, and $S5$ have only one type of neighborhood while D and J each has four different neighborhoods. These two are the most abundant and are likely to be the most favorable places for packing. In the case of Al-Mn quasicrystal, as we shall discuss, these are occupied by Al atoms which also have several different neighborhoods even in the crystalline form of these alloys. Q has two types of neighborhoods but has the smallest area. It is very likely to form structural vacancies. We have made an elaborate calculation to check that these neighborhoods do satisfy the following *exact* sum rule known[21] to be true for any 2D "froth":

$$\sum_n nm(n)p(n) = 36 + \mu_2 , \tag{7}$$

where $m(n)$ is the average number of edges of the cells surrounding a given n-gon.

III. DECORATIONS OF THE 2D PENROSE LATTICE

Having specified the distribution of vertices and their neighborhoods, atomic models can be generated by decorating the 2D PL for a given concentration of (different) atoms. Our strategy is based on the observation that the *local* arrangement of atoms in layers of some

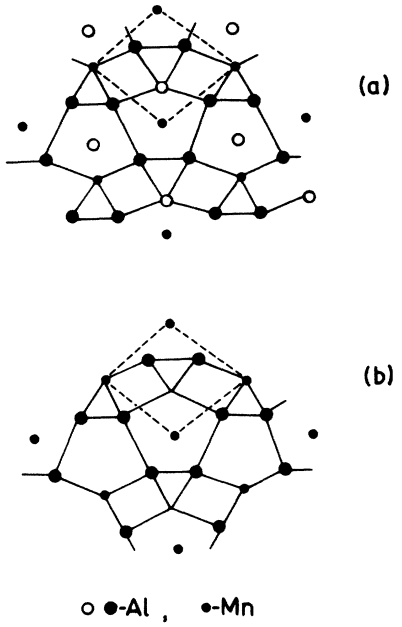

FIG. 3. The two types of layers in the δ-$Al_{11}Mn_4$ structure. As compared to (b), layer (a) has additional Al atoms denoted by an open circle. The dashed lines denote the unit cell of the structure.

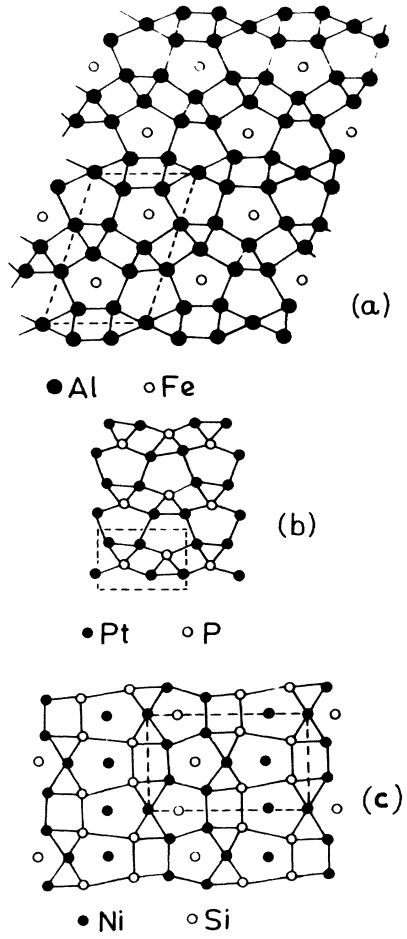

FIG. 4. Layer structures for (a) $Al_{13}Fe_4$, (b) Pt_5P_2, and (c) Ni_3Si_2. The dashed lines denote the unit cell of the structure.

crystalline compounds can also be found in the 2D PL. Moreover, from the fact that the quasicrystal transforms into the corresponding stable crystalline compound, one can expect the local distribution of atoms in quasicrystals to be close to the corresponding crystalline state. Similar conclusions were drawn from one of the Mössbauer[12] and EXAFS (Ref. 13) experiments. Some of the compounds whose layers show similarity with Fig. 2 are δ-$Al_{11}Mn_4$, $Al_{13}Fe_4$ (isostructural with $Al_{13}Co_4$), Pt_5P_2, and Ni_3Si_2. Their layer structures are shown in Figs. 3–5. Several other compounds such as Al_6Mn, α-(Fe-Al-Si), WAl_4, Fe_2Al_5, α-$CuFe_4Al_{23}$, etc. also have[17] layers of the types shown in Fig. 3(b). Comparing these layer structures with Fig. 2, it is easy to see that the hexagonal arrangement of Al atoms around a Mn atom in Fig. 3 is similar to the hexagon shown in Fig. 2. The two pentagons fused at a vertex and forming the polygon with vertices labeled 1–8 in Fig. 2 can be seen in Figs. 4(a) and 4(c) while the polygon with two pentagons joined with a tetragon can be seen in all the three structures in Fig. 4. From this comparison it becomes clear that the packing of pentagons in these alloys (crystalline as well as quasicrystalline) plays an important role. These packings may be done in several ways which may lead to a classification of quasicrystals. We shall focus on two such packings obtained from the 2D PL.

So far there exist no definite rules such as the size of atoms or electron per atom ratio to form quasicrystals. However, if the currently known quasicrystals are considered to be an indication, then alloys having locally icosahedral arrangements or layers with pentagonal arrangements of atoms may be considered[36] to be good candidates. We thus believe that the above-mentioned alloys and others with similar structures should be good candidates for quasicrystal formation. In fact, besides Al-Mn and Al-Fe,[37] α-(Al-Mn-Si) and α-(Al-Fe-Si) (Ref. 11) have already been confirmed to form quasicrystals. However, this structural requirement may not be sufficient or even necessary and only the discovery of many more quasicrystals may lead to certain rules.

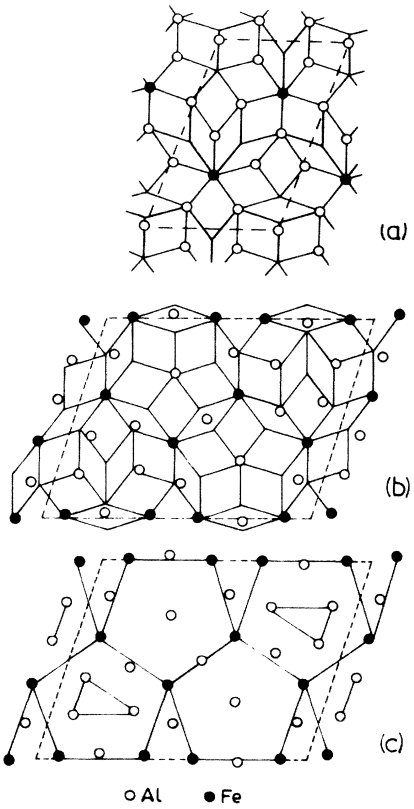

FIG. 5. (a) and (b) show the decoration of the two types of layers in $Al_{13}Fe_4$ by narrow and wide rhombi. In (c) the layer (b) is redrawn with pentagons and thin rhombi as basic units.

In the following we discuss possible decorations of the layers of Al-Mn and Al-Fe having fivefold rotational symmetry and show how such layers can be stacked to generate three-dimensional structures. These should serve as models of the T phase. Though the Al-Mn and Al-Fe quasicrystals fall into the same category, we shall discuss them separately, as their crystalline structures are different.

A. Al-Mn

Consider the δ-$Al_{11}Mn_4$ crystalline structure (Fig. 3). This has two types of Mn layers, while for Al_6Mn there is only one [Fig. 3(b)]. The two layers of δ-$Al_{11}Mn_4$ have chains of pentagons. In one layer [Fig. 3(a)] each Mn atom has five Al atoms as nearest neighbors which form a pentagon, while in the other layer one of such Al neighbors is missing. Since the Al-Mn quasicrystal transforms into Al_6Mn structure upon crystallization, we suggest the following decoration of Fig. 2 by comparing it with the Al_6Mn layer structure. All the vertices in Fig. 2 except a J nearest to $S3$ and $S4$ are occupied by Al atoms. The latter corresponds to having the central vertex in the hexagon shown in Fig. 2 to be vacant, as one finds in the atomic distribution in Al_6Mn layers [Fig. 3(b)]. The centers of the *regular* pentagons are occupied by Mn atoms. These are also the $S3$, $S4$, S, and $S5$ vertices and constitute the second inflation of the original lattice [Fig. 1(a)]. The resulting atomic distribution is shown in Fig. 6(a). This model gives Mn concentration to be 21.7 at. %. From Fig. 6(a) the nearest neighborhoods of (S and $S5$) and ($S3$ and $S4$) are different. The nearest environments of S and $S5$ are similar and have fivefold symmetry [see also Fig. 1(b)]. The concentration of such Mn atoms is $1/\tau^6$. The other two sites $S3$ and $S4$ have nearly identical environments of Al atoms which form a hexagon [the shaded polygons in Fig. 1(b)], similar to the one shown in Fig. 3(b). The concentration of such Mn sites is $1/\tau^5$, and so the ratio of the two kinds of Mn sites is τ which is consistent with the EXAFS (Ref. 13) and one of the Mössbauer[12] data. With this decoration the nearest-neighbor environment of the Mn atoms in each layer is a mixture of the two found in the two layers of δ-$Al_{11}Mn_4$. Also the areas of the four cells which Mn occupies differ at most 2.67% from the mean value. These areas are given in Table I. It is clear that Q and K have the smallest area, and in our model they are vacant. Similar to regular lattices, such sites may be occupied by impurities like B, C, N, O, H, etc., and filling of space by such atoms may even facilitate quasicrystal formation. Al occupies

cells whose areas differ significantly. It will therefore not be surprising if there occurs some relaxation (either in-plane or puckering) around these sites. This will lead to some fluctuation in the interatomic distances. Neglecting such relaxations if a mean distance of 2.5 Å is taken for Al-Mn, then Al-Al distances are 2.93 and 2.5 Å. The latter is also equal to the side of the rhombus. These values lie well within the range found in the crystalline state, where Al-Al distance varies from 2.57 ± 0.03 to 2.89 ± 0.045 Å, and the Al-Mn distance varies between 2.435 ± 0.025 and 2.64 ± 0.03 Å. From this decoration, the nearest-neighbor coordination number of atoms from Voronoi construction ranges from 2 to 5 and therefore the actual crystal structure will contain defects even though the underlying PL is statistically defect free. A slight modification of this decoration can be obtained if the J cells left empty in this decoration are also filled with Al. Then the layer arrangement of atoms will be similar to Fig. 3(a) and the Mn concentration then turns out to be 19.7% with the ratio of the two types of Mn sites still equal to τ. But the distinction between the two sites becomes difficult if only the nearest neighbors are considered. In light of the recent Mössbauer experiments[14] here it should, however, be pointed out that there are more than two types of Mn neighborhoods if atoms beyond nearest neighbors are considered. These can affect the charge distribution around a Mn atom and create different electric fields measured in Mössbauer experiment. Further, the Al-Mn quasicrystal seems to be a two-level system as Mn can occupy either $S3$ and $S4$ or the adjacent J. This fluctuation in the occupancy of $S3$, $S4$, or the J cells may lead to the formation of new local neighborhoods.

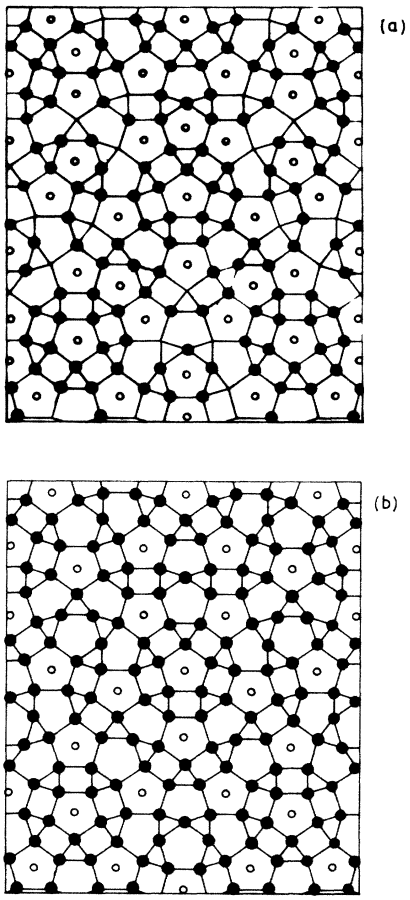

FIG. 6. Decorations of the tetracoordinated lattice (Fig. 2) for layers in (a) Al-Mn and (b) Al-Fe quasicrystals. The solid circles denote Al atoms while the open circles denote Mn (Fe) atoms.

B. Al-Fe

It becomes clear that on the basis of the cell areas, the atomic size cannot be fixed and models based upon hard ball packing may not be very fruitful for these alloys. This can further be expected from the large variation in Al neighbor distances and from the structure of the layers in $Al_{13}Fe_4$, Pt_5P_2, and Ni_3Si_2 shown in Fig. 4. All of them have similar kinds of pentagon-tetragon-triangle nets but the atomic distributions are different. In the case of $Al_{13}Fe_4$ [Fig. 4(a)] alternate pentagons have an iron atom at the center and these are joined together with a tetragon. A similar arrangement on a PL can be obtained[38] if $S3$, $S4$, and $S5$ (shown with circles in Fig. 2) are occupied with iron while D and J are occupied with Al. With this choice those pentagons which join at a vertex have no iron atom at their centers, as also seen in Fig. 4(a). The resulting atomic distribution is shown in Fig. 6(b). All the 20-gons in this case have the same atomic distribution but in general it may be context dependent, as in Fig. 6(a). The coordination number of atoms is 4 or 5 thus indicating the presence of defects in this structure also. This decoration leads to iron concentration of about 14.6 at.%. Experimentally Al-Fe quasicrystal samples have[37] approximately 18 at.% iron. Though there is no published data on the actual Fe concentration in the i phase, it should be noted that the other plane of crystalline $Al_{13}Fe_4$ structure shown in Fig. 5(c) has much higher concentration (32 at.%) of Fe as compared to the one (15.4 at.%) shown in Fig. 4(a). Also though the structure of this plane is based on pentagons, it is quite different from the one shown in Fig. 4(a). It is quite possible that as for regular lattices, successive layers have different atomic arrangements in Al-Fe quasicrystals and in particular in the T phase. Here it is interesting to note that recently two sets of lines have been observed[37] in x-ray powder diffraction from Al-Fe quasicrystals, indicating the presence of planes with spacings d and $2d$.

Henley[11] has decorated one of the layers of $Al_{13}Fe_4$ [Fig. 5(a)] with two kinds of rhombi used in Fig. 1(a). We have decorated the other layer with the same rhombi. Both of these do not belong to the arrowed rhombus pattern. The vertices $D,Q,K,S(S5)$ can be seen on both the patterns though their decorations are different for the two layers. These decorations of a layer with rhombi are *not unique*. We think that instead of decorating a layer with rhombi, it is better to find cells whose distribution may be unique like those shown in Fig. 4 and then to look for corresponding patterns from the PL's. We have found for the other layer of $Al_{13}Fe_4$ a structure based upon pentagons and rhombi, as shown in Fig. 5(c). A prominent

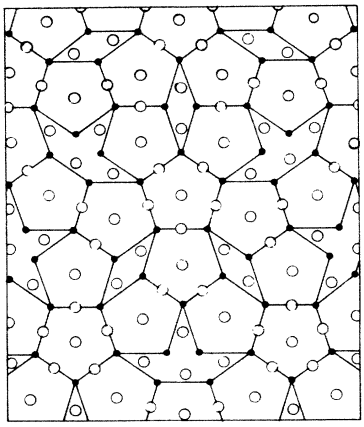

FIG. 7. Atomic arrangement of atoms in layer adjacent to the one shown in Fig. 6. The underlying lattice has been generated from Fig. 2. Open (solid) circles represent Al (Fe) atoms.

feature of this structure is the occurrence of four pentagons with a narrow rhombus in between. A quasiperiodic pattern with similar features can be generated from a suitably decorated 2D PL, and it is shown in Fig. 7. This has been obtained from Fig. 2 by joining points in triangles obtained from perpendicular bisectors. This tiling is full of identical regular decagons. In addition to the prominent unit of the crystalline structure, this has a cap which comes[39] from the three identical double pentagons (fused at a vertex) sharing each other in a 20-gon. This way of generating the structure suggests automatically how to continue it in the third dimension. Looking at the atomic distribution in the crystalline $Al_{13}Fe_4$, an obvious choice is that all these lattice points be occupied with Fe or Mn atoms and each half rhombus has an Al atom. It remains now to show how the centers and the remaining sides of the pentagons should be occupied. In the crystalline structure there are two types of distributions. As shown in Fig. 5(c) there are one or three Al atoms within a pentagon. As the periodicity in a direction perpendicular to the layers is very nearly the same in the crystalline and the T phase, we shall expect both types of pentagons to be necessary also for the T phase. Considering here the simplest case when an Al atom is placed at the center and remaining edges of the pentagons, the Fe concentration turns out to be nearly 35 at.%. The corresponding decoration is shown in Fig. 7. In this decoration each Fe atom is placed on three Al atoms of the underlying layer and an Al atom sits above the tetragon or pentagon of Al atoms. This decoration has the mirror symmetry. The next layer similar to Fig. 6 can be continued on this and thus the average concentration of Fe will be around 25 at.%. Since the period of the structure is 12.4 Å, one would expect some distortions in these layers and two more layers should be added as in the crystalline alloys before the structure repeats itself. Such distortions occur when instead of one, two or three atoms are accommodated within some pentagons. This will also reduce the Fe (Mn) concentration and bring it closer to the experimental value[15] of about 22.4 at.%. When this is done the decorations of the decagons become context dependent and a detailed discussion of this will be published elsewhere.

IV. SUMMARY AND DISCUSSION

In summary we have calculated the distribution of vertices and their near neighborhoods on a 2D PL and suggested its decorations. In contrast to the original quasiperiodic tiling of a plane with "kite" and "dart" or rhombi, these decorations suggest importance of packing of pentagons. Though these have been derived from the arrowed rhombus Penrose pattern, they contain cells which neither have fivefold symmetry nor do their internal angles have any relationship with fivefold symmetry. Most models of i phase have been constructed with packing of icosahedra. As in our case, it is plausible that objects which are not fivefold symmetric could pack to form something with that symmetry.

Our decorations are based upon the crystalline structures of Al_6Mn and $Al_{13}Fe_4$ alloys and should serve as models for the T phase. Though the positions of some of the Al atoms may not be accurate, our model should be a good starting point for more detailed analysis of the T phase. It also becomes clear that there are two types of layers in the T phase, one having almost twice as much the transition-metal atoms as in the other layer. These two layers alternate and such a model is consistent with electron diffraction. A transition from the T phase to the crystalline structure seems to involve rearrangement of atoms within layers such that the chemical order is maintained to a large extent. Our decorations for one of the layers in Al-Mn and Al-Fe quasicrystals differ from one another only in the occupancy of some of the Al and Mn sites. It is likely that different quasicrystals have different concentration of species. Depending upon the actual concentrations and sizes of the atoms, there can be different decorations even though the underlying PL is the same.[40] Al-Mn seems to be a two-level system where Mn can occupy one of the two neighboring sites. The study of the bare and decorated Penrose lattices shows that the actual quasicrystals will in general contain defects which will be arranged in an ordered way and the average coordination number need not be an integer. This is analogous to Frank-Kasper phases.[41] A proper characterization of defects[42] and correlation of our layer arrangements with the atomic distribution in the i phase need further study and we are currently exploring it.

ACKNOWLEDGMENTS

We are thankful to G. Venkataraman for encouragement and critical reading of the manuscript. We also thank M. C. Valsakumar and Rita Khanna for helpful discussions.

[1]D. Shechtman, I. Blech, D. Gratias, and J. W. Cahn, Phys. Rev. Lett. 53, 1951 (1984).

[2]See M. Gardner, Sci. Amer. 236, 110 (1977).

[3]Periodic tiling of a plane can also be generated with two or more unit cells (see Figs. 3, 4, and 5). Our statement excludes such cases as for periodic structures the choice can always be reduced to one.

[4]V. Elser, Phys. Rev. B 32, 4892 (1985) and Acta Crystallogr.

Sect. A **42**, 36 (1986).
[5]D. R. Nelson and S. Sachdev, Phys. Rev. B **32**, 689 (1985).
[6]M. Duneau and A. Katz, Phys. Rev. Lett. **34**, 2688 (1985).
[7]K. M. Knowles, A. L. Greer, W. O. Saxton, and W. M. Stobbs, Philos. Mag. B **52**, L31 (1985).
[8]P. Guyot and M. Audier, Philos. Mag. **B52**, L15 (1985); **B53**, L43 (1986).
[9]M. Kuriyama, G. G. Long, and L. Bendersky, Phys. Rev. Lett. **55**, 849 (1985).
[10]K. Hiraga, M. Hirabayashi, A. Inoue, and T. Masumoto, Sci. Rep. Res. Inst. Tohoku Univ. Ser. A **32**, 309 (1985).
[11]C. L. Henley, J. Non-Cryst. Solids **75**, 91 (1985); V. Elser and C. L. Henley, Phys. Rev. Lett. **55**, 2883 (1985).
[12]L. J. Swartzendruber, D. Shechtman, L. Bendersky, and J. W. Cahn, Phys. Rev. B **32**, 1383 (1985).
[13]E. A. Stern, Y. Ma, and C. P. Bouldin, Phys. Rev. Lett. **55**, 2172 (1985).
[14]M. Eibschutz, H. S. Chen, and J. J. Hauser, Phys. Rev. Lett. **56**, 169 (1986); and Bull. Am. Phys. Soc. **31**, 268 (1986).
[15]L. Bendersky, Phys. Rev. Lett. **55**, 1461 (1985); K. Chattopadhyay, S. Lele, S. Ranganathan, G. N. Subbanna, and N. Thangaraj, Curr. Sci. **20**, 895 (1985).
[16]T. L. Ho, Phys. Rev. Lett. **56**, 468 (1986).
[17]W. B. Pearson, *The Crystal Chemistry and Physics of Metals and Alloys* (Wiley, New York, 1972); see also M. O'Keefee and B. G. Hyde, Philos. Trans. R. Soc. London **295**, 553 (1980) for nets containing pentagon-tetragons-triangles.
[18]N. G. de Bruijn, Ned. Akad. Weten, Proc. Ser. A **43**, 39, 53 (1981).
[19]L. A. Bursill and P. J. Lin, Nature **316**, 50 (1985).
[20]We use PL to be synonymous with the arrowed rhombus pattern given by de Bruijn (Ref. 18).
[21]D. Weaire and N. Rivier, Contemp. Phys. **25**, 59 (1984).
[22]See also A. L. Mackey, Kristallografiya **26**, 910 (1981) [Sov. Phys.—Crystallogr. **26**, 517 (1981)].
[23]D. Levine and P. J. Steinhardt, Phys. Rev. B **34**, 596 (1986); J. E. S. Socolar, P. J. Steinhardt, and D. Levine, *ibid.* **32**, 5547 (1985).
[24]Two tesselations belong to the same PLI class if and only if any finite local pattern in one can be found in the other; for more details, see Ref. 23.
[25]M. C. Valsakumar and V. Kumar, Pramana **26**, 215 (1986).
[26]We use inflated PL to represent a lattice which is similar to the original one but whose cells are bigger (in the present case by a factor of τ) in linear dimensions. The reverse will be true for a deflated lattice.
[27]R. Mosseri and J. F. Sadoc, in *Structure of Noncrystalline Materials,* edited by P. H. Gaskell, J. M. Parker, and E. A. Davis (Taylor and Francis, London, 1983), p. 137.
[28]There are other ways also to define sublattices. For example one can take vertices with the same index 1, 2, 3 or 4 (see the Penrose lattice given in Ref. 18). This leads to two different sublattices. Also in our procedure two types of vertices on each sublattice can be separated out to form eight sublattices.
[29]B. B. Mandelbrot, Y. Gefen, A. Aharony, and J. Peyriere, J. Phys. A **18**, 335 (1985).
[30](a) This also corresponds to removing *D*- and *J*-type vertices on each deflation. (b) After the submission of the manuscript we became aware of the works by M. Jaric (unpublished) and C. L. Henley (unpublished) who have also studied the 2D PL and calculated the frequency of occurrence of different vertices.
[31]This is different from the average coordination of a Voronoi cell. The former is the number of vertices having equal distance (here this is equal to the side of a rhombus) from a given vertex while the latter describes the total number of vertices which are nearer to a given vertex than to any other vertex. It will be worth pointing out that the average electronic density of states of a 2D PL obtained from a nearest-neighbor single *s*-band tight-binding model also shows [T. C. Choy, Phys. Rev. Lett. **55**, 2915 (1985)] features similar to a square lattice even though the local density of states differs from site to site. See also Vijay Kumar and G. Athithan (unpublished).
[32]A. L. Loeb, *Space Structures: Their Harmony and Counterpoint* (Addison Wesley, New York, 1976), p. 23.
[33]By a defective PL we mean a PL which can have vertices other than the eight considered here.
[34]M. Rubinstein and D. R. Nelson, Phys. Rev. B **28**, 6377 (1983); J. P. McTague, D. Frenkel, and M. P. Allen, in *Ordering in Two Dimensions,* edited by S. K. Sinha (North-Holland, New York, 1980), p. 147.
[35]A. Katz and M. Duneau, J. Phys. (Paris) **97**, 181 (1986).
[36]P. Ramachandra Rao and G. V. S. Sastry, Pramana **25**, 225 (1985).
[37]R. Khanna and R. V. Nandedkar, Scr. Metall. **20**, 401 (1986).
[38]It may be noted that Mackay's [A. L. Mackay, Physica **114A**, 609 (1982)] decoration of the 2D PL is essentially the same. He, however, took in his decoration all the atoms of the same type.
[39]We encourage the reader to take a photocopy of Fig. 7 on a transparency and superimpose it on Fig. 2 or Fig. 6.
[40]C. L. Henley and V. Elser, Philos. Mag. Lett. **B53**, L59 (1986).
[41]F. C. Frank and J. S. Kasper, Acta Crystallogr. **11**, 184 (1958); **12**, 483 (1959).
[42]See also, R. Mosseri and J. F. Sadoc, J. Non-Cryst. Solids **75**, 115 (1985).